

Supplementary Material: Two-directional Image Retargeting with Region-Aware Texture Enhancement

Dubok Park
dubok.park@samsung.com

Samsung Research,
Samsung Electronics,
Seoul, South Korea

1 Qualitative Results

1.1 Visual Comparison for Figure 10 in Paper

To validate the effectiveness of propose approach, visual comparison results of RetargetME [1] are presented here.



Figure 1: Visual comparison for “jon” ($\Phi_{out} = 0.5 \times \Phi_{in}$).

Figure 1 shows the visual comparison for “jon” image (50% aspect ratio reduced). SC [2] shows the discontinuities which are due to the pixels being excessively removed. SM [3], SNS [4], and WARP [5] provide a severe cut or distortion on snowman and boy which is important content. SV [6] and MOP [7] show visually pleasing results without severe distortion. However, proposed method shows more reliable result for snowman with fine detail compared to the existing methods.

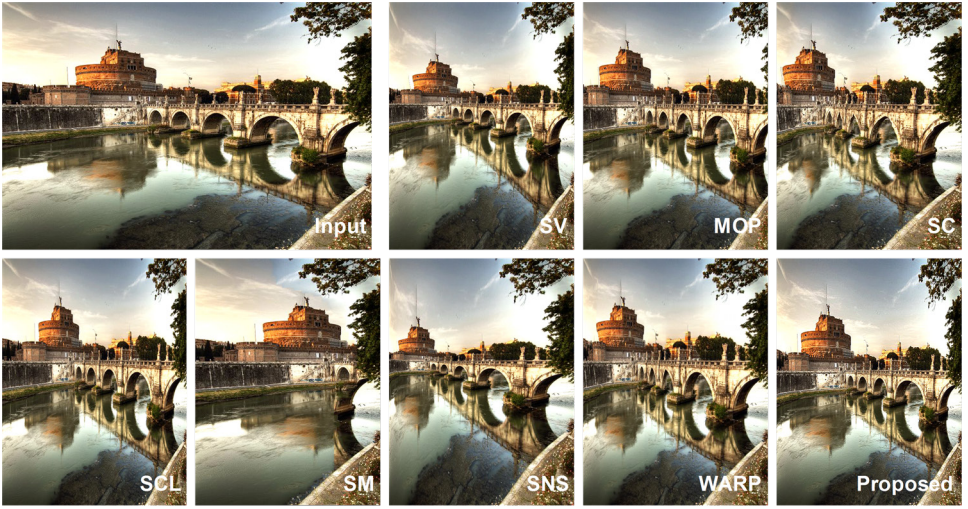


Figure 2: Visual comparison for “SetAngle” ($\Phi_{out} = 0.5 \times \Phi_{in}$).

Figure 2 shows the visual comparison for “SetAngle” image (50% aspect ratio reduced). SV, SC, and WARP shows the shape distortion on brown stadium (left-side is slanted) and SM provides a severe cut of the bridge. Although SNS shows the reliable result entirely, brown stadium is resized too small. Proposed method shows better result for brown stadium and bridge overall.



Figure 3: Visual comparison for “Woman” ($\Phi_{out} = 1.33 \times \Phi_{in}$).

Figure 3 shows the visual comparison for “Woman” image (33% aspect ratio increased). MOP, SC, and SM include a severe distortion on vase (pixels being excessively removed or distorted). Furthermore, picture frames in SM are dislocated (one parallel to the other in input image). Although SNS provides well-preserved picture frame, the lower part of woman is cut out. Similarly, picture frame in WARP is cut out, even though it retains the shape of woman. Although, picture frames and vase in proposed result are stretched from the input image, proposed method provides well-preserved woman without severe distortion.

1. 2 Visual Comparison for Figure 12 in Paper

Figure 4 shows the results of “brick_house” image (50% aspect ratio reduced). Cycle-IR [8] contains shape distortion (slightly bending) at the roof as shown in blue rectangle. Without this distortion, proposed method provides content-preserving result and fine details in grass.

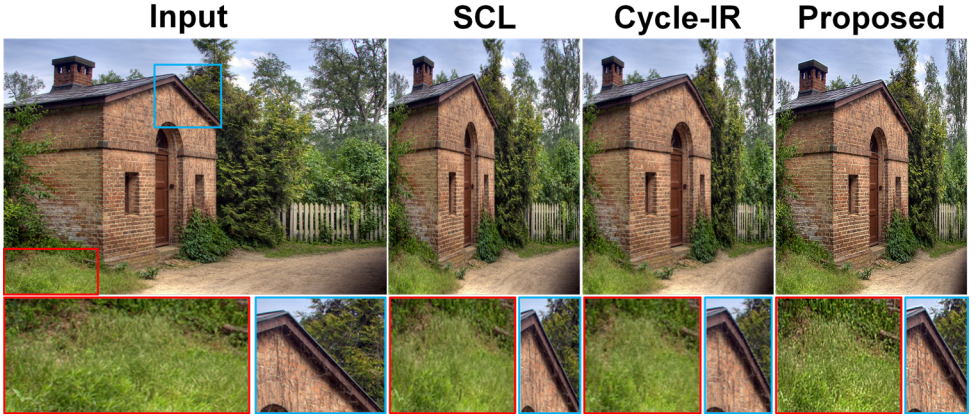


Figure 4: Visual comparison for “brick_house” ($\Phi_{out} = 0.5 \times \Phi_{in}$).

Figure 5 shows the results of “housefence” image (50% aspect ratio reduced). Although Cycle-IR provides better for house than SCL, it has some artifacts in fence, such as shape distortion and over-smoothing as shown in close-up images. On the other hand, proposed method shows visually pleasing result with salient edges and details while preserving house since the target image is generated by region-aware guidance map which contains input salient shape.

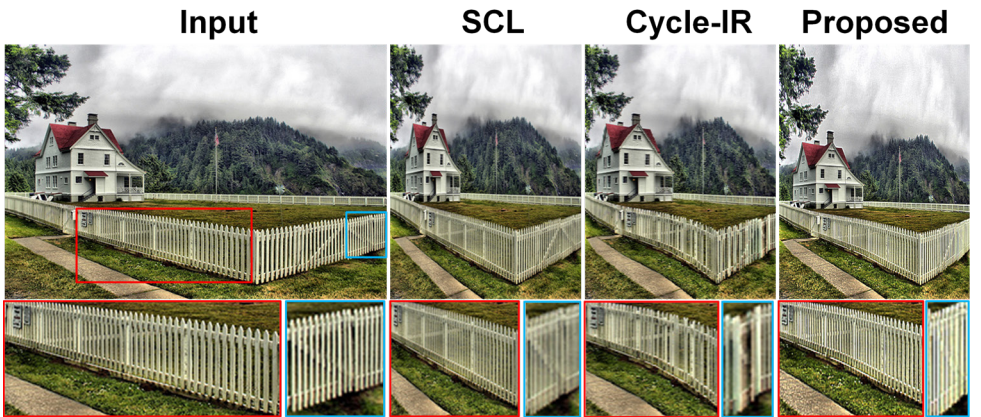


Figure 5: Visual comparison for “housefence” ($\Phi_{out} = 0.5 \times \Phi_{in}$).

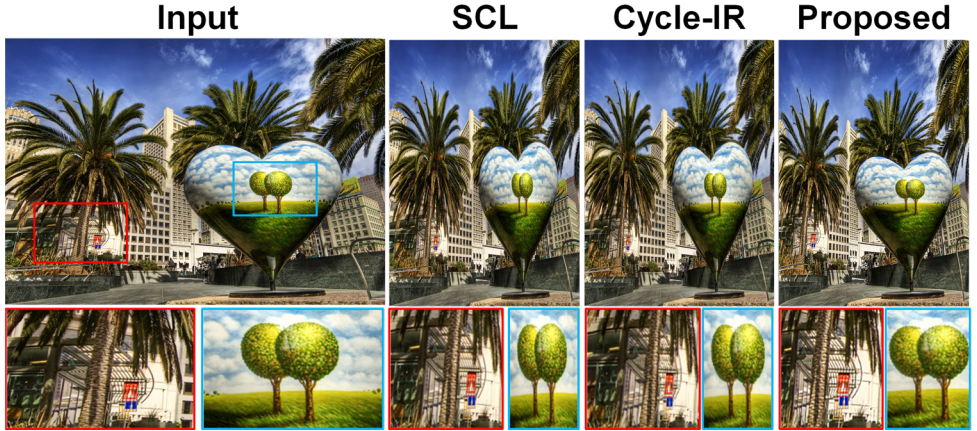


Figure 6: Visual comparison for “Sanfrancisco” ($\Phi_{out} = 0.5 \times \Phi_{in}$).

Figure 6 shows the results of “Sanfrancisco” image (50% aspect ratio reduced). Proposed approach maintains the thin lines in red rectangle while these lines are over-smoothed and twisted in Cycle-IR. Furthermore, proposed method shows better result for trees in blue rectangle than SCL and Cycle-IR.

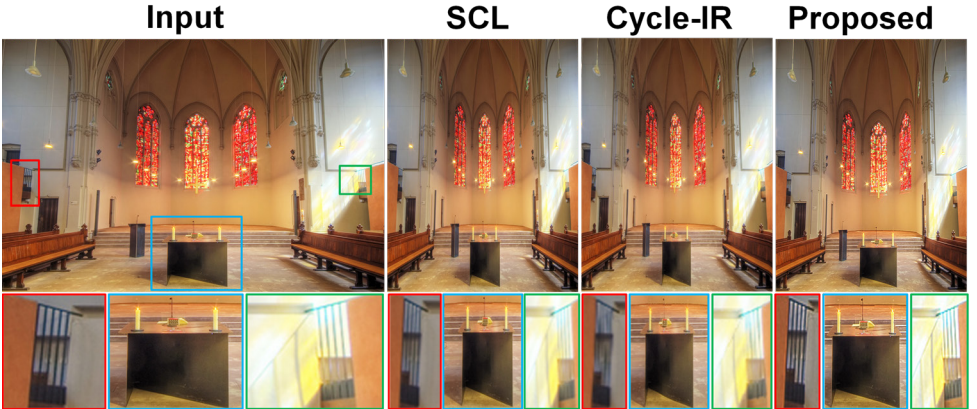


Figure 7: Visual comparison for “Johanneskirche” ($\Phi_{out} = 0.5 \times \Phi_{in}$).

Figure 7 shows the results of “Johanneskirche” image (50% aspect ratio reduced). Proposed approach preserves the thin lines in red rectangle and green rectangle while these lines are over-smoothed and twisted in Cycle-IR. Also, Cycle-IR contains shape distortion at the bottom of table as shown in blue rectangle.

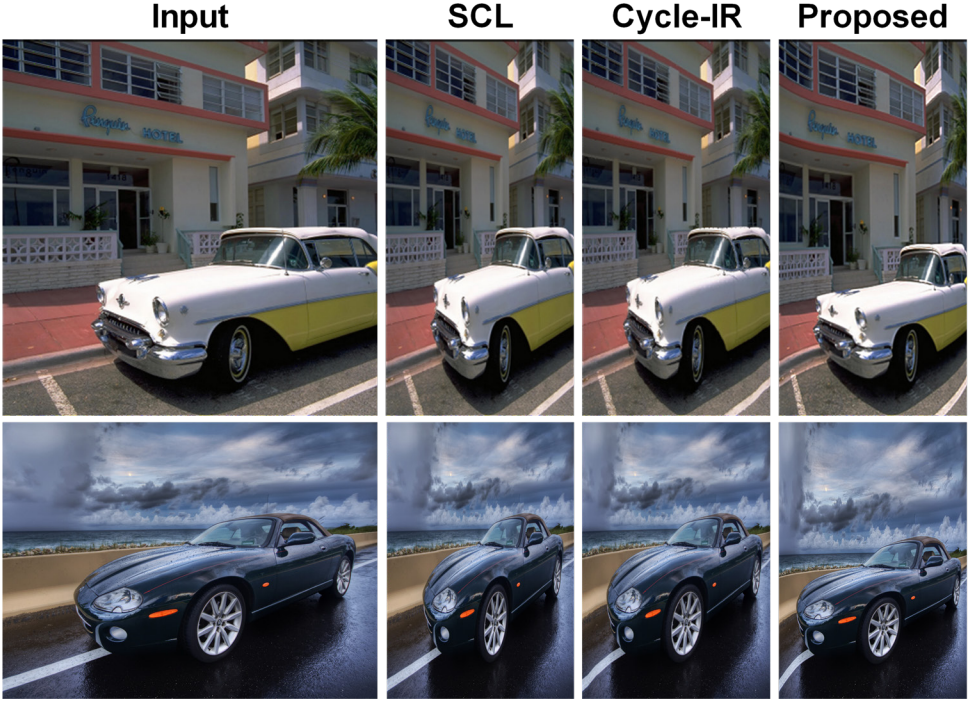


Figure 8: Visual comparison for “car1” (up), “car” (bottom), ($\Phi_{out} = 0.5 \times \Phi_{in}$).

Figure 8 shows the results of “car1” and “car” images which show that the ARS scores of proposed method are lower than Cycle-IR in Figure 12 of paper. Proposed method shows bent structure (windows of 2nd floor in “car1”) and line (white line in “car”) although Cycle-IR provides well-preserved structure. These result in lower scores in ARS measures. It is one of the limitation case of proposed method since proposed method has no consideration for global consistency and spatial coherence. Thus, spatial coherence between the input and retargeted image may help the proposed approach to achieve better performance.

2 Refinement Filters for Importance Map

Figure 9 shows refined results of importance map via proposed approach and guided filter [9]. Proposed approach and guided filter take about 500ms and 76ms, respectively, to refined initial importance map of 360×640 image (MATLAB implementation on Intel Core i7, 4.2GHz CPU and 64GB RAM). Although guided filter shows the low computational complexity, it contains halo near edges as shown in close-up of Figure 9.

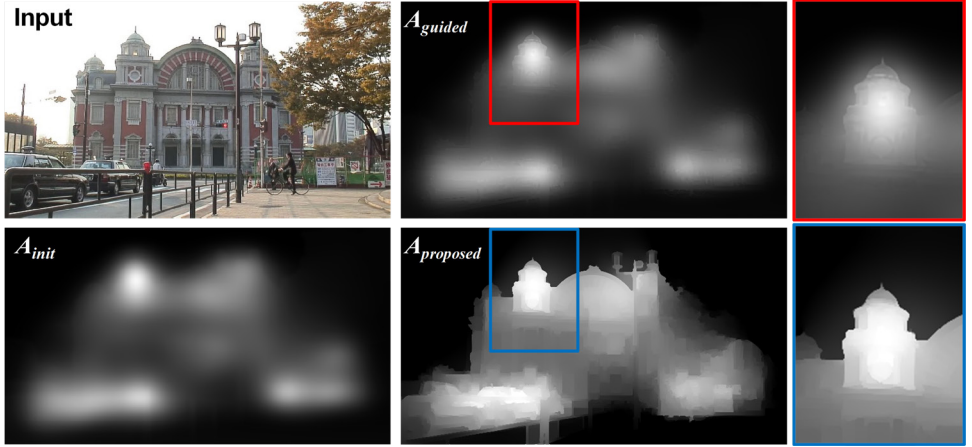


Figure 9: Visual comparison with refinement filters.

3 Ablation Study

In order to provide a better insight into the overall approach, ablation experiments are presented here to show how each component of proposed method affects performance. Aspect ratio of input image is 75% reduced to show difference of each result effectively. Figure 10(d) is the result of two-directional non-uniform scaling via estimated scaling ratio while Figure 10(b), (c) are the results of non-uniform scaling without two-directional scaling ratios (vertical or horizontal only). Butterfly in Figure 10(b) is too squeezed with respect to the horizontal direction while that of Figure 10(c) shows a distortion of plant at the bottom left of image. On the other hand, two-directional non-uniform scaling resizes the input image for each direction properly, which provides content-preserving result as shown in Figure 10(d). Furthermore, region-aware guidance enhances fine details of the retargeted image as shown in Figure 10(e). Likewise, proposed approach operates properly “surfer” image as shown in Figure 11.

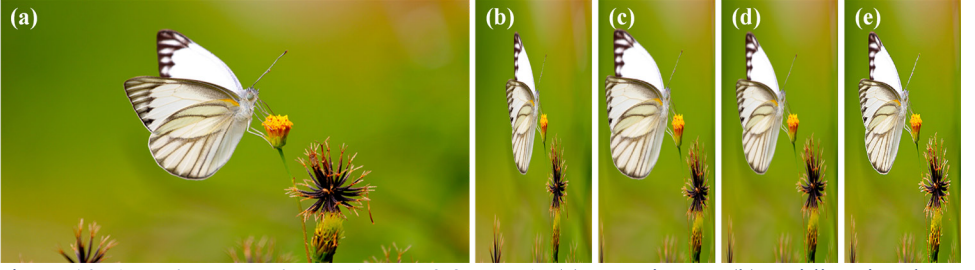


Figure 10: **Ablation experiment ($\Phi_{out} = 0.25 \times \Phi_{in}$).** (a) Input image. (b) Unidirectional non-uniform scaling ($\varphi_x=0, \varphi_y=1$). (c) Unidirectional non-uniform scaling ($\varphi_x=1, \varphi_y=0$). (d) Two-directional non-uniform scaling without region-aware guidance ($\varphi_x=0.558, \varphi_y=0.442$). (e) Two-directional non-uniform scaling with region-aware guidance.

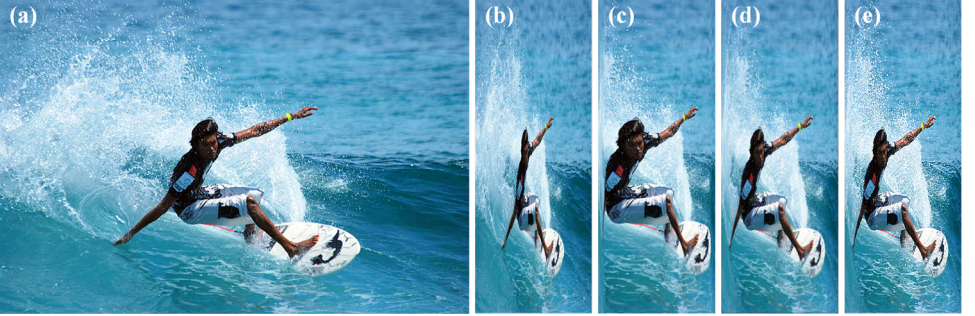


Figure 11: **Ablation experiment ($\Phi_{out} = 0.25 \times \Phi_{in}$).** (a) Input image. (b) Unidirectional non-uniform scaling ($\varphi_x=0, \varphi_y=1$). (c) Unidirectional non-uniform scaling ($\varphi_x=1, \varphi_y=0$). (d) Two-directional non-uniform scaling without region-aware guidance ($\varphi_x=0.577, \varphi_y=0.423$). (e) Two-directional non-uniform scaling with region-aware guidance.

References

- [1] M. Rubinstein, D. Gutierrez, O. Sorkine, and Ariel Shamir. A comparative study of image retargeting. *ACM Trans. on Graph. (ToG)*, vol. 29, no. 6, Dec. 2010.
- [2] M. Rubinstein, A. Shamir, S. Avidan. Improved Seam Carving for Video Retargeting. *ACM transactions on graphics (ToG)*, vol. 27, issue 3, Aug. 2008.
- [3] Y. Pritch, E. Kav-Venaki, and S. Peleg. Shift-map image editing. In *Proc. ICCV*, 2009.
- [4] Y.S. Wang, C. L. Tai, O. Sorkine, and T. Y. Lee. Optimized Scale-and-stretch for Image Resizing. *ACM Trans. on Graph. (ToG)*, vol. 27, issue 5, 2008.
- [5] L. Wolf, M. Guttman, and D. Cohen-Or. Non-homogeneous content-driven video-retargeting. In *Proc. ICCV*, Oct. 2007.
- [6] P. Krahenbuhl, M. Lang, A. Hornung, and M. H. Gross. A system for retargeting of streaming video. *ACM Trans. Graph. (ToG)*, vol. 28, no. 5, 2009.
- [7] M. Rubinstein, A. Shamir, and S. Avidan. Multi-operator media retargeting. *ACM Trans. on Graph. (ToG)*, vol. 28, no. 3, pp. 23:1–23:11, 2009.
- [8] W. Tan, B. Yan, C. Lin, and X. Niu. Cycle-IR: Deep Cyclic Image Retargeting. *IEEE Transactions on Multimedia*, vol. 22, issue 7, pp. 1730–1743, July 2020.

- [9] K. He, J. Sun, and X. Tang. Guided Image Filtering. *IEEE Transactions on Pattern Analysis and Machine Intelligence*, doi: 10.1109/TPAMI.2012.213.